Swelling of a polymer brush probed with a quartz crystal resonator

Arno Domack,[1] Oswald Prucker,[2] Jürgen Rühe,[1] and Diethelm Johannsmann[1,*]
[1]*Max-Planck Institute for Polymer Research, P.O. Box 3148, 55021 Mainz, Germany*
[2]*Department of Chemical Engineering, Stauffer III, Stanford University, Stanford, California 94305-5025*
(Received 13 November 1996; revised manuscript received 7 March 1997)

We have studied the temperature dependence of swelling of a polystyrene brush in cyclohexane with quartz resonators and ellipsometry. The swelling of the layer, which has been covalently bound to a silicon oxide surface, continuously increases as the temperature is raised. The data from the quartz resonator display a ''film resonance,'' which indicates that the thickness of the brush is on the order of the wavelength of transverse sound. The quantitative analysis shows that the acoustic thickness as determined with the quartz resonator is higher than the optical thickness from ellipsometry. We argue that this difference is partly due to the high contrast achieved in acoustical measurements, which makes the quartz resonator most sensitive to dilute regions in the tail of the segment density profile. The relation between the acoustic thickness and the hydrodynamic thickness is discussed. [S1063-651X(97)03307-2]

PACS number(s): 62.80.+f, 68.45.Nj, 83.10.Nn, 83.85.−c

INTRODUCTION

Polymers that have been terminally grafted onto a solid surface by a covalent chemical bond have recently attracted much interest both because of their importance in the context of surface modification and colloid stabilization as well as due to the fundamental questions about the structure and the dynamics of polymers constrained in this peculiar way. Of special interest are so-called polymer brushes in which the graft density of surface attached chains is so high that they have a strong overlap between neighboring chains leading to a conformation in which the polymer is elongated normal to the surface [1,2]. The field has been extensively reviewed in Refs. [3–7]. From the fundamental side, considerable theoretical [8–15] and experimental [16–21] effort has gone into the determination of the segment density profile $\rho(z)$ as a function of coverage, molecular weight, polydispersity, solvent quality, and surface curvature. Neutron scattering [16–18] and reflection [19–21] have been the most widely employed methods. While the segment density profile certainly is a fundamental characteristic of the polymer brush, it is not always clear how the interaction of a brush with, for instance, an opposing solid wall [22], an atomic force microscope (AFM) tip [23], another brush [22], and a shear flow of solvent [24–27] is determined by the density profile. Given the considerable experimental effort in determining a segment density profile, it seems worthwhile to probe the behavior of the brush under external stimuli such as shear flow directly. The behavior under shear in particular is of high importance because it relates to the tribological [27–29], rheological [30], and hydrodynamic [26] behavior.

In this study we report on the response of a polymer brush to transverse acoustic waves. The behavior of polymer brushes under strong shear recently has been subject to considerable debate. It is predicted [31] and confirmed by experiment [32] that shear will change the structure of the brush and induce an increase in thickness. This scenario is not expected for brushes on quartz resonators because of the low shear strain (~1%) and the fast time scale (<1 μs). Our data show indeed that linear acoustics is observed, thereby definitely excluding shear thickening.

The brush is grown on a quartz resonator, slightly changing the frequencies and bandwidths of its resonances. For a thin brush in air, the changes in the resonances are mainly determined by the mass [33]

$$\delta f = -\frac{f f_f}{2 Z_q} m, \tag{1}$$

with δf the frequency shift, f the frequency of the given harmonic, f_f the fundamental frequency, $Z_q = 8.8 \times 10^6$ kg m^{-1} s^{-2} the acoustic impedance of quartz, and m the mass per area. The central approximation in using quartz crystals as ''microbalances'' is that the wavelength of shear sound inside the film is much longer than its thickness. This limit obviously breaks down when the brush becomes highly swollen and dilute. When the brush is much thicker than the wavelength of shear sound (or its decay length), the viscosity or the complex shear modulus of the brush can be derived from the frequency shift according to [34]

$$\delta f + i\,\delta\Gamma = \frac{i f_f}{\pi Z_q}\sqrt{\rho G} = \frac{(i-1)}{\sqrt{2}}\frac{f_f}{\pi Z_q}\sqrt{\rho\omega\eta}, \tag{2}$$

with $2\delta\Gamma$ the change in bandwidth, ρ the density, $G = G' + iG''$ the shear modulus, and η the viscosity. It turns out that there is a very interesting situation in between the limits of a very thin film [Eq. (1)] and a very thick film [Eq. (2)], where the brush thickness is about one-quarter of the wavelength of sound. For this situation, termed ''film resonance'' [33–35], the bandwidth goes through a maximum. A film resonance is very useful for acoustic characterization because the acoustic thickness can be determined. The acoustic thickness is the depth z where most of the shear sound is

*Author to whom correspondence should be addressed.
FAX: 49-6131-379 360.
Electronic address: johannsmann@mpip-mainz.mpg.de

reflected. The significance of the acoustic thickness is not obvious when the viscoelastic properties vary gradually across the brush-solvent interface as it is expected for a swollen brush. As we will show below, the derived acoustic thickness is higher than the ellipsometrically derived thickness. One reason is that shear sound tends to be reflected at the outer edge of the brush. Because the acoustic thickness critically depends on details of the segment density profile in the tail of the distribution, it is difficult to relate it to a density profile as determined with neutron scattering. However, other types of interaction such as repulsion between two polymer brushes [22] or the hydrodynamic behavior [24–26] depend on the tail of the profile in a very similar way as the acoustic thickness. In particular, the acoustic thickness is closer to the hydrodynamic thickness than the ellipsometric thickness. The acoustic thickness therefore is a useful quantity for assessing the interactions of brushes.

The brushes investigated were prepared by the ''grafting from'' technique [38–41], in which the polymer is formed *in situ* at the surface of the substrate by radical chain polymerization from a self-assembled monolayer of an initiator. The brush thickness achievable with this technique exceeds those from ''grafting to'' procedures, where preformed polymers are reacted with appropriate surface sites. This is due to the fact that the limiting factor is the diffusion of monomers towards a growing chain rather than diffusion of polymers to the surface. Following the grafting from approach, polymer molecules with molecular weights up to several 10^6 g/mol can be attached to the surfaces with high graft densities and films with thicknesses of several hundred nanometers (in the dry state) can be obtained. The molecular weights of the polymers can be measured after cleaving an ester bond, which is part of the anchor group connecting the polymer to the surface [38–40].

Here we investigate the behavior of a brush in poor solvent and around the θ condition. A polystyrene brush was immersed in cyclohexane and the temperature was varied between 10 °C and 60 °C. The solvent quality of polystyrene in cyclohexane improves with temperature, the θ point for unbound polystyrene in cyclohexane being at $T_\theta = 34\,^\circ\mathrm{C}$ [42]. The brush is in the concentrated solution regime for all temperatures. It is expected to be swollen at high temperatures and more compact below T_θ. Around the θ temperature, mean-field calculations [10,43] as well as simulation studies [11,14] predict a gradual collapse of the brush. Our data confirm that prediction.

THEORY

The formalism underlying our analysis of frequency shifts and bandwidths has been described elsewhere [36,44]. We summarize the results and describe the adaptation of the general formalism to the particular experimental situation of a polymeric adsorbate in a liquid environment. The generalized acoustic impedance Z^* at an interface is defined as

$$Z^*(\omega) = \frac{\sigma(\omega)}{\dot{u}(\omega)}, \tag{3}$$

with σ the shear stress, u the particle displacement, and $\dot{u}$ the particle velocity. All quantities are complex numbers. For a traveling acoustic wave in a bulk medium, the generalized impedance Z^* is the same as the conventional acoustic impedance $Z = \rho v$, with v the speed of sound. When several waves contribute to the stress, σ is the sum of the shear stress exerted by all waves, including the waves reflected inside the sample. In this sense, Z^* is clearly not a material constant but depends on geometry.

With this definition, the frequency shift of a quartz resonator in contact with a viscoelastic medium is written as

$$\delta f^* = \frac{i f_f}{\pi} \frac{Z^*}{Z_q}, \tag{4}$$

where $\delta f^* = \delta f + i\,\delta\Gamma$ is the shift of complex resonance frequency $f^* = f + i\Gamma$ and 2Γ is the bandwidth. The shear stress exerted by a single wave is

$$\sigma = iGku, \tag{5}$$

with $k = \omega(\rho/G)^{1/2}$ the wave vector. In a geometry with shear waves traveling in both directions, we get

$$Z^* = G_f \frac{ik(u_+ - u_-)}{i\omega(u_+ + u_-)} = \sqrt{\rho G_f}\,\frac{1-r}{1+r} = Z_f \frac{1-r}{1+r}, \tag{6}$$

with u_+ and u_- the amplitudes of waves traveling forward and backward, $r = u_-/u_+$ the normalized amplitude of the reflected wave at the quartz surface, and $Z_f = (\rho_f G_f)^{1/2}$ the acoustic impedance of the film at the quartz surface. Z_f is understood as a material constant, not as a generalized impedance in the sense of Eq. (3). Equation (6) shows that calculating the frequency shift δf^* of a resonator in a viscoelastic medium requires the knowledge of the acoustic impedance at the quartz surface and the amplitude of shear sound reflected inside the sample.

An important feature appears when the reflectivity r in Eq. (6) approaches -1. This is, for example, the case when the sample is a homogeneous film with a thickness d_f equal to a quarter of the wavelength of sound λ. In this case the bandwidth 2Γ of the resonances becomes large and the frequency shift δf changes sign. Note that a positive frequency shift δf corresponds to a negative apparent mass of the film if it is interpreted in the naive picture of the quartz crystal microbalance. An acoustic model is required to correctly analyze the behavior of quartz resonators once the film thickness is comparable to the wavelength of sound. A situation where r in Eq. (6) is close to -1 has been termed film resonance [35] because the film itself forms a resonator that has an eigenfrequency close to the driving resonators frequency. When the two coupled resonators (quartz and film) have similar frequencies, the transfer of energy into the film is most efficient and the damping of the quartz resonance reaches a maximum. Film resonances are unambiguously identified when the frequencies and bandwidths are measured on several harmonics. The condition $d_f \sim \lambda/4$ will only be fulfilled on those harmonics where the wavelength approximately matches four times the film thickness. These harmonics have large bandwidths and the frequency shift changes sign for harmonics lower and higher than the resonant ones.

The feature of the film resonance has been exploited in the past to measure the viscoelastic shear moduli of thin

films under various conditions such as hydroplastification, swelling in a solvent, heating, and irradiation with uv light [37,45,46]. In these situations the film was homogeneous and the ambient medium was air or vapor.

Here we report on a film resonance observed in a liquid environment. Naturally, the film resonance is highly damped. The interface between the film and the liquid environment may be smeared out. Also, the phase of reflection at the brush-solvent interface will be different from 0°. Reasonably simple analytic expressions for the frequency shift can be given if a viscoelastic box profile is assumed. We get

$$\delta f^* = \frac{i f_f}{\pi} \frac{Z_{\rm br}}{Z_q} \frac{(Z_{\rm br}+Z_l)\exp(2ik_{\rm br}d_{\rm br})-(Z_{\rm br}-Z_l)}{(Z_{\rm br}+Z_l)\exp(2ik_{\rm br}d_{\rm br})+(Z_{\rm br}-Z_l)}, \quad (7)$$

with $Z_{\rm br}$ and Z_l the acoustic impedance of the brush and the liquid, $k_{\rm br}$ the wave number inside the brush, and $d_{\rm br}$ the thickness of the brush. The denominator becomes large when $\exp(2ik_{\rm br}d_{\rm br}) \sim -1$. This is again the condition for a film resonance. For swollen brushes the condition $k_{\rm br}d_{\rm br} \sim \pi/2$ or $d_{\rm br} = \lambda/4$ does not exactly match the maximum of $\delta\Gamma$ because the factor $Z_{\rm br}$ depends on swelling as well. Still the condition $d_{\rm br} = \lambda/4$ can serve as a good first guess.

For more general viscoelastic profiles numerical procedures are needed. Most conveniently, the samples is divided into N slabs of thickness d_i with a local acoustic impedance $Z_i = (\rho_i G_i)^{1/2}$ and a local wave number k_i. The situation is analogous to the calculation of reflections and transmissions of multilayer structures in optics, where the acoustic impedance Z takes the place of the refractive index [47]. Note, however, that in contrast to the refractive index, Z can vary over many orders of magnitude. The contrast in shear-acoustic experiments is thus much higher than in optics.

In calculating the reflection amplitude r [Eq. (6)] we follow the ''matrix formalism'' [48]. At any depth z_i of the sample, the amplitudes of the waves going forward and backward are written as a vector $u = (u_{+,1} u_{-,i})$. In accordance with the conventions in optics, we take the direction of the z axis as pointing towards the quartz surface. All time-dependent quantities vary as $\exp(i\omega t)$. The outermost layer, which is the liquid, has index 0. In the liquid, there is no wave going towards the sample surface, i.e., $u_0 = (1,0)$.

The reflection coefficient at the quartz surface is $r = u_{-,N}/u_{+,N}$. The propagator P connecting u_N to u_0 is defined by

$$u_N = P \cdot u_0 = L_N \cdot S_{N,N-1} \cdot L_{N-1} \cdot \cdots \cdot L_1 \cdot S_{1,0} \cdot u_0, \quad (8)$$

with L_i the layer propagator of the ith layer,

$$L_i = \begin{bmatrix} \exp(ik_i d_i) & 0 \\ 0 & \exp(-ik_i d_i) \end{bmatrix}, \quad (9)$$

and $S_{i,i-1}$ the interface propagator between layer i and $i-1$,

$$S_{i,i-1} = \frac{1}{2} \begin{bmatrix} 1+Z_{i-1}/Z_i & 1-Z_{i-1}/Z_i \\ 1-Z_{i-1}/Z_i & 1+Z_{i-1}/Z_i \end{bmatrix}. \quad (10)$$

Given a decay length of transverse sound at megahertz frequencies in liquids of typically less than 1 μm, it is safe to assume that there are no waves reflected from the cuvette walls. We neglect longitudinal contributions, which if present can cause problems because they have a different impedance and can propagate to the cuvette wall and be reflected there [46,49]. However, longitudinal waves would not go unnoticed. Because they depend on the position of the sample in the cell, strong longitudinal contributions would prevent the reproducibility of the measurements.

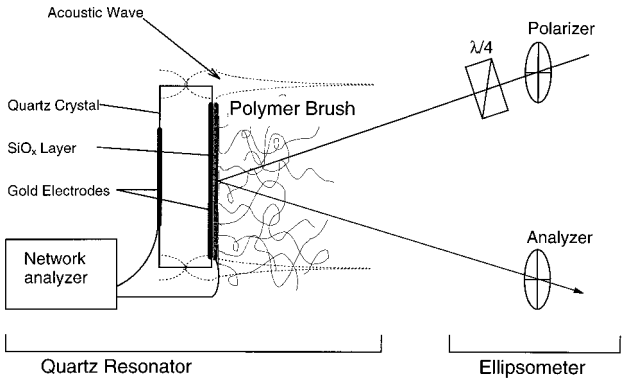

FIG. 1. Experimental setup. The polymer brush is attached to the surface of the quartz resonator and changes its resonance frequencies and bandwidths during swelling in a solvent of varying quality. The ellipsometric thickness is determined in parallel. The dashed lines show the amplitude of the acoustic wave. The thickness of the brush has been largely exaggerated for the purpose of illustration.

While the calculation of the frequency shift δf^* from a given viscoelastic profile is straightforward, the inversion of a given experimental set of frequency shifts and bandwidths to the shape of the viscoelastic profile is not without ambiguities. It is therefore crucial to identify qualitative features, which can be interpreted without recursion to quantitative fitting. The film resonance is the most prominent of those features. When the film resonance occurs, it is safe to assume that there is a reflecting interface (with some finite interface width) somewhere inside the sample. The sound waves reflected from that interface have acquired an overall phase of π. The width of the film resonance will depend on the loss tangent $\tan\delta = G''/G'$ in the medium as well as the nature of the interface. If the interface is smooth or if the acoustic contrast is low, a large fraction of the energy will be transmitted. Therefore, the acoustic energy inside the brush decreases and the Q factor of the film resonance is low.

For frequencies far away from the film resonance, the frequency shift δf^* is dominated by the prefactor $Z_{\rm br} = (\rho G_{\rm br})^{1/2}$ in Eq. (7). Therefore, the shear modulus (both $G'_{\rm br}$ and $G''_{\rm br}$ at the quartz surface can be independently assessed.

EXPERIMENT

A sketch of the experimental setup is shown in Fig. 1. We employed AT-cut quartz crystals with a diameter of 1.4 cm and a fundamental frequency of 4 MHz. The surfaces were plane parallel and optically polished. The back electrode had a keyhole shape to achieve energy trapping [50]. Effects from the mounting structure can be assessed in the following way. First, the quartz is held with an alligator clamp and the

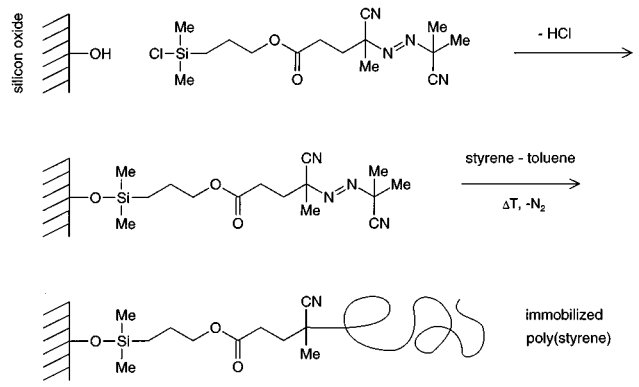

FIG. 2. Schematic depiction of the synthesis. The initiator is self-assembled on the surface of an evaporated oxide layer. The polymer grows by free radical polymerization from that surface-bound initiator.

frequencies and bandwidths are determined on all harmonics. When the quartz is mounted in the liquid cell, the rim of the quartz is covered with a silicone glue to prevent electrical contact between the front and the back. This mounting structure affects only the lowest harmonics. The frequency shift induced by the mounting is less than 10^{-5} of the reference frequency and therefore much less than the shifts induced by swelling of the brush. Only low harmonics are sensitive to the mounting because the confinement of the oscillation to the central area is more effective for short wavelengths of sound.

The front electrode covered the whole surface of the quartz. A 30-nm layer of SiO_x was evaporated onto the gold electrode to provide the oxidic surface needed for the synthesis of the polymer brush. Both the electrodes and the SiO_x layer are sufficiently hard to be considered as a part of the quartz crystal for all purposes of acoustic modeling.

The amplitude of shear sound at the quartz surface is in the range of tens of nanometers. Given a wavelength inside the brush on the order of micrometers, we derive a shear strain on the order 1%. Note, however, that the shear rate is quite high due to the high frequency. We checked for any acoustic nonlinearities by varying the driving voltage of the impedance analyzer. A dependence of frequency on the driving voltage would have been indicative of shear thinning [51] or shear thickening as it was found with the surface forces apparatus [28,49,52]. More basically, the fact that the resonances are nice Lorentzians in itself proves that linear acoustics is observed. When we sweep through the resonance, the amplitude of oscillation increases from zero to its maximum value. If there were shear thickening, the frequency of resonance would depend on amplitude and the Lorentzians would be distorted. Since we appear to be in the range of linear acoustics, we conclude that the structure of the brush is unperturbed by shear [27,53–55].

The synthesis of the polymer brushes followed the grafting from approach as depicted in Fig. 2. Details are described in Refs. [38–41]. Briefly, the first step is the immobilization of an initiator for free radical polymerization at the surface. The initiator used was a derivative of 920-bis-isobutyronitrile (AIBN), which was attached to the SiO_x surface via a silane moiety. Subsequently, the polymerization is thermally initiated in the presence of styrene monomer. The concentration of styrene was 50 vol % in toluene. After polymerizing for 15 h at 60 °C, the sample was rinsed with solvent, underwent Soxhlet extraction overnight, and was dried in 10^{-3} mbar at 60 °C for 6–14 h. The dry thickness of the resulting polystyrene film was ellipsometrically determined to be 70 ± 3 nm. The molecular weight of this particular sample could not be detected since the amount of material is too small to be used for polymer analysis. However, from other experiments using large substrates as well as high surface area silica gels, where similar polymerization conditions have been chosen, we can estimate that the molecular weight of the sample is in the range $M_n\sim(0.5-0.8)\times10^6$ g/mol [38,39]. The polydispersity M_w/M_n is about 2. From the molecular weight and the mass density (i.e., mass per area) the distance between two anchoring sites is calculated to be 30–40 Å. Frequently, this is expressed as a grafting density σ, where the minimum geometric area per segment is divided by the area per chain. In molecular-dynamics simulations this corresponds to the fraction of surface sites occupied by polymer chain ends. A value of $\sigma=0.03-0.06$ results.

It has been suggested that collapsed films may be unstable with respect to lateral structure formation [11,56,57]. The stability criteria given in Ref. [56] indicate that high-molecular-weight brushes are particularly good candidates for such a scenario. In order to investigate that possibility, we looked at the dry films with a scanning force microscope. We found that the rms roughness of the film surface was less than 3 nm in all cases. For thin films, this roughness is most likely due to the SiO_x film, which has considerable roughness due to the evaporation process. In any case, the rms roughness is much less than the film thickness. If a lateral instability occurs its amplitude is much less than the film thickness (cf. Fig. 6 in Ref. [56]). For matters of viscoelastic modeling, we consider the lateral variation of thickness as weak and neglect it in the following. This assumption is also supported from the neutron reflection data, which indicate that the brush-solvent interface is quite sharp (see below).

RESULTS

Figure 3 shows the normalized frequency shifts $\delta f/f$ and the normalized shifts in bandwidths $\delta\Gamma/f$ for ten harmonics between 12 and 84 MHz. We usually discard data from the fundamental (4 MHz) because of insufficient energy trapping. First, the data very clearly show the feature of the film resonance. Because higher harmonics have shorter wavelengths, the films resonance occurs at low thickness (i.e., low temperature). This result in itself is quite remarkable because one might have doubted the applicability of the one-dimensional acoustic model for such a complicated acoustic situation. Also, it is far from obvious that the brush-solvent interface is sharp enough to be considered as an acoustic interface. It seems natural that the film resonance is highly damped. The reasons for the low Q factor are twofold: First, the medium inside the resonator is viscous and dissipates energy and second the reflectivity of the brush-solvent interface may be low either because of low acoustic contrast or because it has a large intrinsic interface width.

We have observed a continuous change of thickness in all experiments but one. A continuous collapse is predicted from mean-field calculations [10,43] and simulations [4]. In one

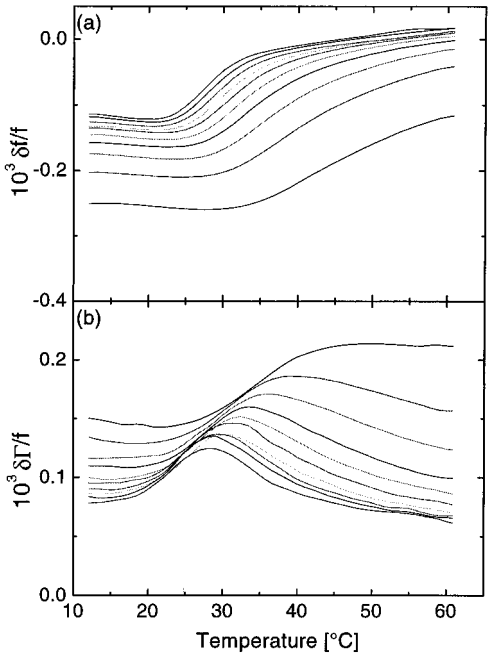

FIG. 3. Frequency shifts and bandwidths for the quartz-brush system immersed in cyclohexane as a function of temperature. The thickness increases with increasing temperature. At a certain thickness ($d_{br} \sim \lambda/4$) a ''film resonance'' occurs.

preliminary experiment, which could not be reproduced, a discontinuous drop in the interfacial acoustic impedance at 27 °C occurred [58]. We do not discuss the this finding in the following.

Because the condition of a film resonance involves the ratio of the thickness d_{br} and the wavelength λ_{br}, it is of great help to get independent information on d_{br} and λ_{br}. In order to assess the thickness during swelling we performed *in situ* ellipsometric measurements. Because of the low contrast between polystyrene and cyclohexane, only the ellipsometric parameter Δ varies significantly. When converting Δ to an ''optical thickness'' we used a box profile for the refractive index. Figure 4 shows the derived swelling ratio

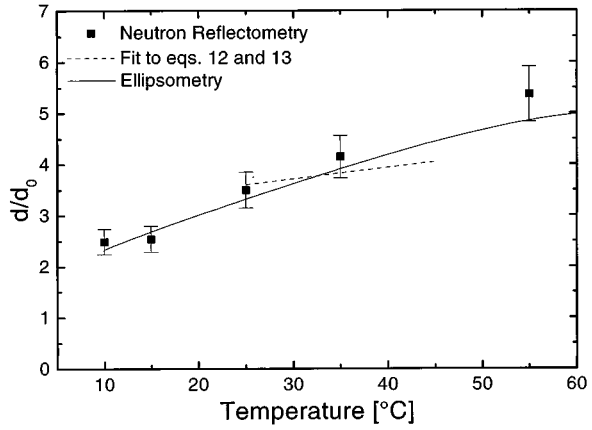

FIG. 4. Swelling ratios d/d_0 as determined with ellipsometry and neutron reflection. A box profile was used in the analysis of the ellipsometry data. The solid squares are data obtained on an identical brush with neutron reflectometry [59]. The dashed results from applying Eqs. 12 and 13 from Ref. [10] to our experiment.

d/d_0 as a function of temperature. One could call the resulting thickness an ''equivalent optical thickness.'' It should be kept in mind that the box profile is an input to the optical analysis. More realistic profiles will display a gradual decrease in the segment density. We chose the error function for modeling because this is the simplest functions having both the thickness d and the interface width w as adjustable parameters. Note that parabolas are not appropriate because our samples are polydisperse [61]. We emphasize that at no point in our subsequent discussion do we rely on details of the functional form of the segment density. When modeling our profiles with an error function

$$\varphi_p(z) = \varphi_0 \frac{1}{2}\left[\frac{1}{2} - \mathrm{erf}\left(\frac{z-d}{w}\right)\right], \tag{11}$$

with d the thickness, w the interface width, and φ_0 a normalization constant, we found that the thicknesses d derived from ellipsometry depends on the interface width w. In this case w is an input parameter, $w=0$ corresponding to a box profile. The optical thickness, therefore, is not model independent.

In a previous experiment [59], the thickness of a similar polystyrene brush was measured with neutron reflectometry. Weakly swollen brushes ($\chi > 0.5$) showed a good contrast between the layer and solvent. The reflectivity curves could be well fitted with error functions with $w < 0.1d$. Unfortunately, the contrast for neutron reflection from highly swollen brushes ($\chi < 0.5$) and/or the instrumental resolution at these large length scales was so low that no detailed information about the profile could be obtained. The thickness given in Fig. 4 was determined from the spacing of the fringes. Within the experimental error, the data from ellipsometry and neutron reflection are consistent.

Karim *et al.* [19] have previously investigated similar polystyrene brushes in cyclohexane. They used a molecular weight $M_w = 105\,000$, a dry thickness of 10 nm, and a dimensionless grafting density of $\sigma = 0.027$. From Fig. 2 in Ref. [19] the degree of swelling at 31.5 °C is around 3, which is consistent with our results. Generally speaking, their segment density profile appears to be smoother than the ones obtained in our experiments. The difference may be due to the fact that our molecular weight was about a factor of 10 higher than the one used by Karim *et al.* At high molecular weights the fluctuations due to the finite size of the chain decrease [14]. The edge observed for our samples at the θ condition are certainly sharper than what mean-field calculations [8–10] predict. Interestingly, the molecular-dynamics studies [14] show a deviation from the mean-field picture for high molecular weights at the θ temperature, the outer edge being sharper as well (Fig. 8 in Ref. [14]). Polydispersity should smoothen the profile [60,61]. However, this argument may not be effective under poor solvent conditions.

It is interesting to compare the experimental thickness with the detailed predictions made by Zhulina *et al.* [10] which were generated with a mean-field approach. Zhulina *et al.* predict the thickness of a brush at the θ condition to be

$$H_\theta = \frac{4}{\pi}\left(\frac{wp}{2}\right)^{1/4} \sigma^{1/2} N a, \tag{12}$$

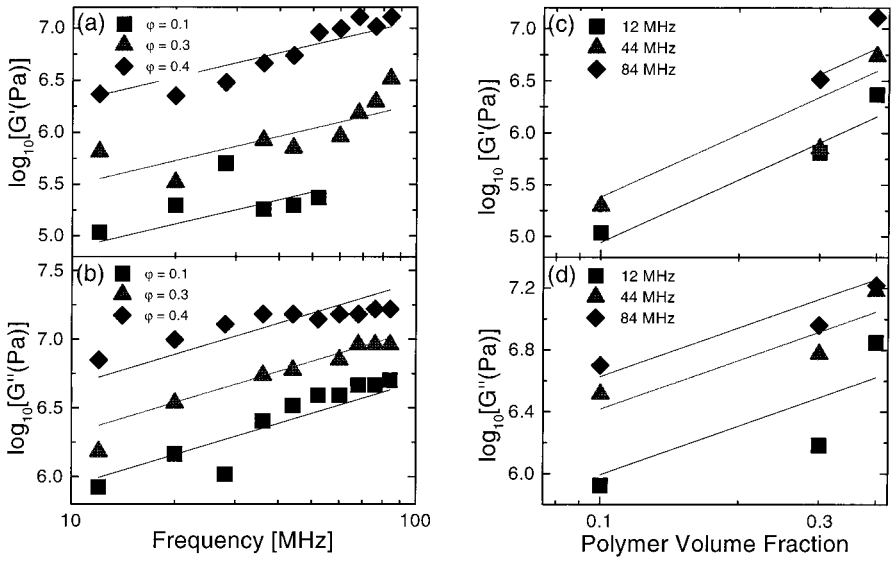

FIG. 5. Frequency shifts and bandwidths obtained for a quartz immersed into bulk solutions of polystyrene in cyclohexane at $T=24\,^{\circ}\mathrm{C}$. The dotted lines are fits to the equations $G'(\varphi_{\mathrm{PS}},\omega)=G_0'(f/50\ \mathrm{MHz})^{\alpha'}(\varphi_{\mathrm{PS}}/0.3)^{\beta'}$ and $G''(\varphi_{\mathrm{PS}},\omega)=G_0''(f/50\ \mathrm{MHz})^{\alpha''}(\varphi_{\mathrm{PS}}/0.3)^{\beta''}$.

with H_θ the thickness at the θ temperature, w the dimensionless third virial coefficient, p the dimensionless parameter measuring the chain stiffness [5], σ the grafting density, N the degree of polymerization, and a the length of one segment. Note that the variable σ has a different meaning in Ref. [10]. The slope of the thickness versus height close to the θ temperature is

$$\frac{dH}{dT}=H_\theta\frac{v_0}{T_\theta}\frac{2}{3\pi}\left(\frac{p}{2}\right)^{1/4}w^{-3/4}\sigma^{-1/2}, \tag{13}$$

where we have used $v=v_0(T-T_\theta)/T_\theta$. For polystyrene we have $p\sim 1.7$ and $a\sim 2.5$ Å. There is some uncertainty about the degree of polymerization N and the dimensionless grafting density σ. We estimate the degree of polymerization N to be between 5000 and 8000, yielding σ between $\sigma=0.03$ and $\sigma=0.06$. The third virial coefficient w is derived from the relation $w=\frac{1}{3}-\chi_1$, where $\chi_1=0.149$ [42] describes the concentration dependence of the χ parameter ($\chi\sim\chi_0+\chi_1\varphi+\cdots$). For a degree of polymerization of $N=7000$, Eq. (12) matches our data at the θ temperature best. The slope dH/dT is then determined without adjustable parameters. These calculations are indicated as a dashed line in Fig. 4.

In principle, it would be highly desirable to obtain independent information on the wavelength of sound λ as well. Such measurements are in principle questionable because there are by definition no bulk samples equivalent to a polymer brush that could be used to independently derive the shear modulus. However, due to the high frequency we believe that concentrated polymer solutions are a good first approximation. At low frequencies, polymer solutions are much different from brushes because they can flow, whereas the brush cannot. In the megahertz region the entanglements that presumably are present both in the brush and in the concentrated polymer solutions prevent flow regardless of whether or not there is terminal attachment to a substrate. Both the brush and the concentrated polymer solution are ''transient networks.'' The *ns* dynamics mostly takes place at the level of polymer strands in between entanglements. In the blob picture, the brush properties are similar to the bulk properties up to the size of the blobs, which is in the range of several nanometers. Therefore, we used concentrated polymer solutions in contact with the quartz resonator to independently assess the wavelength λ.

The wavelength λ depends on both the frequency ω and local segment density φ_{PS} via the dependence of the shear modulus G on ω and σ_{PS}. To obtain $\lambda(\sigma_{\mathrm{PS}},\omega)=2\pi/\omega[G(\sigma_{\mathrm{PS}},\omega)/\rho]^{1/2}$, one needs to measure the shear modulus G of the bulk material as a function of volume fraction of polymer σ_{PS} and frequency ω. The density ρ depends weakly on σ_{PS}. Viscoelastic measurements on polymer solutions in that frequency range have been performed with ultrasonic reflectometry [62,63]. Unfortunately, we are not aware of any data on the polystyrene-cyclohexane system. We determined $G(\varphi_{\mathrm{PS}},\omega)$ with a quartz resonator immersed into a polystyrene-cyclohexane solution. This measurement is equivalent to ultrasonic reflectometry apart from the fact that resonators are used instead of transducers and detectors. It is not obvious that the interfacial region probed by evanescent wave of the quartz has the same viscoelastic properties as the bulk because there may be either polymer adsorption or polymer depletion at the quartz surface [5]. Such surface anomalies are a general impediment when ultrasonic reflectometry is used to test bulk viscoelastic parameters. However, the thickness of an anomalous surface layer (adsorbate or depletion layer) should be roughly equal to the correlation length of concentration fluctuations in the bulk medium [64]. For concentrated solutions, this correlation length is only a few monomers and therefore much smaller than the penetration depth of the evanescent wave. The quartz resonator should essentially probe bulk properties.

Figures 5(a) and 5(b) show the elastic and viscous moduli G' and G'' of bulk solutions at a volume fraction of $\varphi_{\mathrm{PS}}=0.1$, 0.3, and 0.4 as a function of frequency. The straight

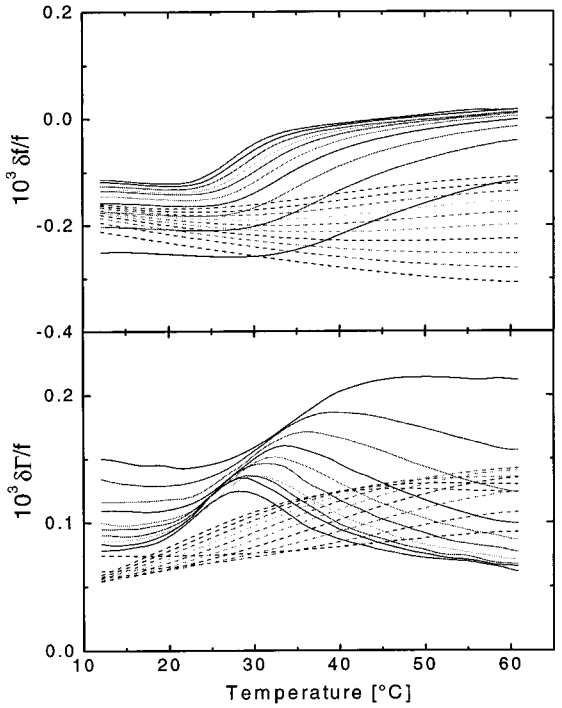

FIG. 6. Viscoelastic modeling of the polymer brush according to Eq. (7). The dashed lines are theoretical data, which use a viscoelastic box profile with the ellipsometric thicknesses from Fig. 4 and viscoelastic parameters determined for bulk polymer solutions (Fig. 5). This model contains no free parameters. The occurrence of a film resonance is reproduced. A comparison with the experimental data (straight lines, same as Fig. 3) shows that the position of the film resonance is predicted incorrectly.

lines are power laws according to $G'(\varphi_{\mathrm{PS}},\omega)=G_0'(f/50\ \mathrm{MHz})^{\alpha'}$ and $G''(\varphi_{\mathrm{PS}},\omega)=G_0''(f/50\ \mathrm{MHz})^{\alpha''}$. Figures 5(c) and 5(d) show some of the same data (12, 44, and 84 MHz) plotted versus density. In this case the power laws (straight lines) do not work as well. For a thorough analysis more detailed measurements, preferably as a function of temperature, have to be made. At this point we confine ourselves to a simple model, which can be readily implemented into the modeling of the polymer brush. We use power laws for the concentration dependence as well and write $G'(\varphi_{\mathrm{PS}},\omega)=G_0'(f/50\ \mathrm{MHz})^{\alpha'}(\varphi/0.3)^{\beta'}$ and $G''(\varphi_{\mathrm{PS}},\omega)=G_0''(f/50\ \mathrm{MHz})^{\alpha''}(\varphi/0.3)^{\beta''}$. The derived values are $G_0'=2.4$ MPa, $\alpha'=0.77$, $\beta'=2$, $G_0''=8.8$ MPa, $\alpha''=0.75$, and $\beta''=1.04$. The deviation between this fit and the data is below a factor of 2. Since G enters the wavelength of sound only as a square root, this error does not affect the subsequent discussion.

With independent information on both the thickness d and the wavelength of sound λ, one can model the experiment without any adjustable parameters. The dotted lines in Fig. 6 show the modeled data (dashed lines), when a viscoelastic box profile with the optical thickness and the bulk viscoelastic shear moduli is used. The model qualitative reproduces the occurrence of a film resonance. However, the position of the film resonance is quite wrong. Either the wavelength of sound or the acoustic thickness has been determined incorrectly.

We see two possible candidates at the origin of the discrepancy. First, the shear modulus of a brush could indeed be much lower than the shear modulus of a polymer solution of equivalent density. Due to chain stretching the number of entanglements or the response of chains to stress could be different. Note, however, that these peculiarities would have to be operative at the local scale. Also, the square-root dependence of the wavelength on the shear modulus would require that the difference between polymer solutions and bulk polymers is at least a factor of 4. A factor of 4 in G, on the other hand, is hardly compatible with our data. It moves the overall scale of frequency shifts by a factor of 2 due to the prefactor in Eq. (7).

A second possible origin of the discrepancy is a failure of the box profile to accurately describe the experiment. Especially in the swollen state, smoother functions such as the error function [Eq. (11)] are certainly more appropriate. However, when using error function profiles to model the data, we found that for every choice of parameters, a certain box profile could be found, which gave very similar results. When a very smooth profile was used, the equivalent box profile had a large thickness. Box profiles can reproduce our data surprisingly well provided that the acoustic thickness is chosen to be much higher than the optical thickness. This peculiar behavior originates from the very strong dependence of acoustic contrast on the segment density.

Figure 7 illustrates the situation. Figure 7(a) shows the segment density profiles for four different error functions with identical thickness d but interface widths w varying between $w=0.2d$ and $1.4d$. Figure 7(b) shows the amplitude of an optical p-polarized wave as it approaches the gold surface and is reflected. This is the behavior of one of the two optical waves used in ellipsometry. When the interface becomes smoother, the profile of the optical amplitude becomes smoother as well, but qualitatively follows the density profile. In particular, the ''reflection depth'' z_r, where most of the light is reflected, remains approximately constant. The contrary is true for the acoustic wave displayed in Fig. 7(c). The reflection depth z_r, where most of the sound wave is reflected, now depends on the interface width. The reason that optical and acoustical waves behave so differently is the widely different contrast. While the refractive index (the ''optical impedance'') [47] changes by only a few percent, the acoustic impedance varies by some orders of magnitude. The reflectivity at an impedance step is determined by the normalized impedance difference (optical or acoustical) rather than the impedance difference itself. For the optical case that is easily verified by $r=(n_1-n_2)/(n_1+n_2)\sim\Delta n/2n$. Incremental reflectivities at impedance gradients therefore depend on $dZ/2Z=\frac{1}{2}d(\ln Z)$. This consideration is unimportant for the optical case because the refractive index n varies by only a few percent. The acoustic impedance, on the other hand, varies over some orders of magnitude. Therefore, the logarithm of the impedance is the relevant quantity rather than the impedance itself.

The consequences are seen in Fig. 7(c). For this model calculation it was assumed that the shear modulus depends on the square of the segment density. In all cases, the sound amplitude can be reasonably approximated by a box profile. However, different thicknesses of the equivalent boxes (''acoustic thicknesses'') have to be used for the different interface widths. For an interface width $w\sim1.4d$ the acous-

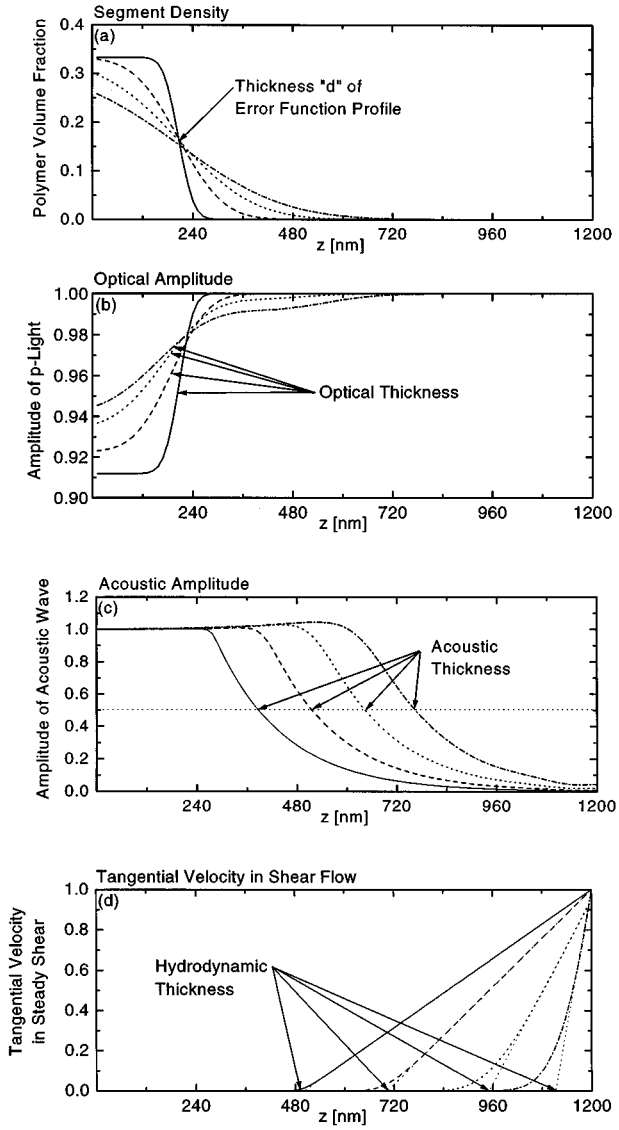

FIG. 7. Influence of (a) the segment density profile onto (b) the profile of light amplitude and (c) shear sound amplitude. Error functions with an interface width between $w=0.2d$ and $1.4d$ were used. While the light amplitude profile matches the density profile, the sound amplitude decays at a depth much larger than d. The position of the steepest gradient z_{rf} is the ''reflection depth,'' which will roughly be reproduced when fitting the data with box profiles. The figure illustrates that the acoustic thickness is larger than the optical thickness. The origin of that discrepancy is the high contrast in acoustics. (d) shows the tangential velocity in stationary shear flow calculated according to Ref. [24]. The derived hydrodynamic thickness is even higher than the acoustic thickness.

tical wave is reflected at a depth corresponding to about $3d$. Most of the wave is reflected at the outer edge of the brush. For a sharp interface ($w\sim 0.2d$), on the other hand, the factor is only about 1.5.

It seems interesting to compare this situation with other experiments, where one is interested in how a stationary shear flow of liquid above the brush is influenced by the brush. That problem has been treated in the frame of hydrodynamic screening by Anderson and co-workers [24,25]. They start from the Brinkman equation

$$\eta\nabla^2 v-\nabla p-\eta\kappa^2 v=0, \tag{14}$$

with η the viscosity, v the velocity of the medium, p the pressure, and κ^2 the hydrodynamic screening parameter, which is related to the mesh size [64]. When the pressure p is assumed to be constant, the flow is in the x direction, and all gradients are along the z direction we get the ordinary differential equation

$$\frac{\partial^2 v}{\partial z^2}=\kappa^2 v, \tag{15}$$

which has to be solved under the boundary conditions

$$\begin{aligned} v&=0 \quad \text{at } z=0,\\ \partial v/\partial z&=1 \quad \text{at } z=\infty. \end{aligned} \tag{16}$$

Unfortunately, we are not aware of experiments where $\kappa^2(\varphi_{\mathrm{PS}})$ has been determined for the polystyrene-cyclohexane system. For the purposes of illustration and comparison with Ref. [25], we adopt the data derived for the poly(α-methylstyrene)-cyclohexane system [25,65], which are $\kappa=3.45\times 10^7\,[\rho(g/\mathrm{cm}^3)]^{0.858}\,\mathrm{cm}^{-1}$. Figure 7(d) shows the profiles of tangential velocity derived from numerical integration of Eq. (15). The hydrodynamic thickness is derived from extrapolating the linear range down to zero velocity. Hydrodynamic thicknesses of 490, 700, 950, and 1120 nm are found for the interface widths of $w=0.2d$, $0.6d$, d, and $1.4d$, respectively. The acoustic thicknesses derived from the acoustic amplitude profile are about 380, 520, 650, and 770 nm. The acoustic thickness apparently is lower than the hydrodynamic thickness.

These considerations [Fig. 7(c) in particular] explain why the differences between a smooth profile and a box profile with a large depth are hard to distinguish. As a consequence, we fit all our data with box profiles. This is not to be understood in the sense that we assume the density profile to be rectangular. All we say is that the acoustic behavior of smooth profiles can be well approximated by box profiles, where the thickness of the box depends on the smoothness of the segment density profile. If the segment density profile was known to be an error function, one could derive a relation between the interface width w and the thickness of the box profile yielding equivalent results. This relation would, however, critically depend on the functional form of the profile. Since the error function is just a guess, such a relation would be of very limited validity.

In order to improve the quality of the model, we allowed the acoustic thickness to vary by introducing a ratio R_{ao} between the optical thickness and the acoustic thickness. R_{ao} is allowed to depend on the temperature as $R_{ao}=R_0(T_\theta)+R_1(T-T_\theta)$. The two parameters R_0 and R_1 put the film resonances into the right place and adjust the spacing between the film resonances on the different harmonics. Figure 8 shows the results obtained with that model. The resulting parameters are $R_0(T=T_\theta)=1.85$ and $R_1=0.028\ ^\circ\mathrm{C}^{-1}$. $R_{ao}(60\ ^\circ\mathrm{C})$ comes out to be 2.5.

Note that Fig. 8 contains only two fit parameters. Naturally, the fit is worst at temperatures far away from the film resonance, i.e., at the highest and lowest temperatures. Substantial further improvement can be achieved by allowing more parameters to vary. Explicit use of error functions in

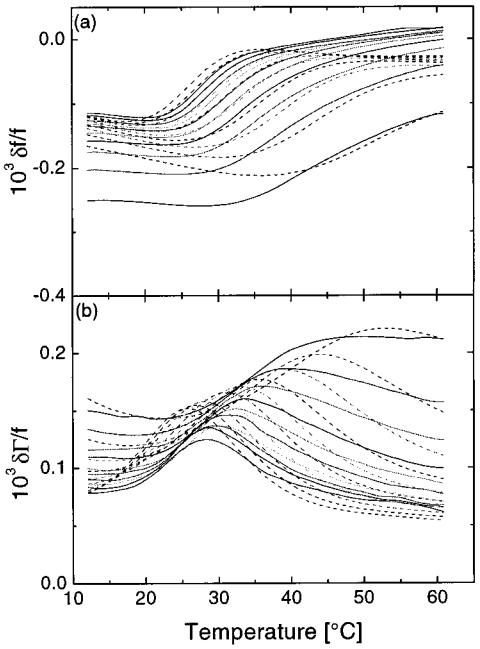

FIG. 8. Fit to the data of Fig. 3 with a model accounting for the difference between optical and acoustic thickness by introducing a factor $R_{ao}(T_\theta=1.85)$ and $R_{ao}(T=60\ ^\circ\mathrm{C})=2.5$.

the acoustic modeling also helps. Unfortunately, the various input parameters to a more realistic model interfere with each other. In order to model the system more realistically more theoretical input on the viscoelastic behavior would also be needed. At this point we confine ourselves to the qualitative features, which do not rely on details of the theory.

Finally, we want to recall that there are in principle two reasons for the surprisingly high acoustic thickness. It could be that the megahertz shear modulus of a brush is much lower than the shear modulus of a polymer solution at the same segment concentration. It could also be that the smoothness of the profile in conjunction with the large acoustic contrast moves the acoustic interface into the dilute tail of the brush. Obviously, both effects can operate simultaneously. We think that the second mechanism certainly contributes for two reasons. First, ascribing the whole effect to an anomalously low shear modulus would change the overall scale of the frequency shifts by a factor of 2 through the prefactor in Eq. (7). This is hardly compatible with our data. Second, a smooth profile is expected for polymer brushes and the above analysis showed that the shear waves will very generally be reflected at the outer egde. Our data do not allow us to state to what extent an anomalously low shear modulus contributes. We again want to emphasize that the experiments happen in the linear regime and that the shear induced distortion of the brush's structure are minute.

In the future we want to investigate the variation of acoustic thickness with grafting density. Another interesting question would be to investigate brushes with strong intermolecular interaction, namely, polyelectrolyte brushes. The optical and the acoustic behavior of these systems may be quite different.

CONCLUSION

We have measured the temperature dependence of swelling for a polystyrene brush in cyclohexane with a quartz resonator. The occurrence of a film resonance is very useful for diagnostic purposes because it allows us to determine the acoustic thickness of the brush. We have used measurements on polymer solutions in contact with the quartz resonator to independently assess the wavelength of the shear sound in the brush. The acoustic thickness derived in this way is higher than the optical thickness by about a factor of 2. The difference between acoustic and optical thickness gets larger for higher temperatures. One source of the discrepancy may be that the shear modulus of a brush is much lower than the shear modulus of a polymer solution of the same concentration. A second source certainly is the fact that the acoustic contrast is much higher than the optical contrast. The acoustic waves are mostly reflected in the dilute outer tail of the segment density distribution. This situation is reminiscent of investigations on the hydrodynamic thickness of polymer brushes, which is also largely determined by the outermost fraction of the brush. Simple model calculations show that the acoustic thickness should be some what lower than the hydrodynamic thickness.

ACKNOWLEDGMENTS

We thank Steve Granick, Ekaterina Zhulina, and Gary Grest for helpful discussions.

[1] S. Alexander, J. Phys. (France) **38**, 983 (1977).
[2] P. G. deGennes, J. Phys. (France) **37**, 1443 (1976).
[3] I. Szleifer and M. A. Cariggnano, Adv. Chem. Phys. **94**, 165 (1996).
[4] G. S. Grest and M. Murat, in *Monte Carlo and Molecular Dynamics Simulations in Polymer Science*, edited by K. Binder (Clarendon, Oxford, 1994).
[5] G. J. Fleer, M. A. Cohen Stuart, J. M. H. M. Scheutjens, T. Cosgrove, and B. Vincent, *Polymers at Interfaces* (Chapman and Hall, London, 1993).
[6] A. Halperin, in *Soft Order in Physical Systems*, Vol. 323 of *NATO Advanced Study Institute, Series B: Physics*, edited by Y. Rabin and R. Bruinsma (Plenum, New York, 1994), p. 33.
[7] A. Halperin in, A. Halperin, M. Tirell, and T. P. Lodge, Adv. Polym. Sci. **100**, 31 (1991).
[8] S. T. Milner, T. A. Witten, and M. Cates, Macromolecules **21**, 2610 (1988).
[9] D. F. Shim and M. E. Cates, J. Phys. (France) **50**, 3535 (1989).
[10] E. B. Zhulina, O. V. Borisov, V. A. Pryamitsyn, and T. M. Birshtein, Macromolecules **24**, 140 (1991).
[11] P.-Y. Lai and K. Binder, J. Chem. Phys. **97**, 586 (1992).
[12] F. M. Haas, R. Hilfer, and K. Binder, J. Chem. Phys. **102**, 2960 (1995).
[13] A. Milchev and K. Binder, Macromolecules **29**, 343 (1996).

[14] G. S. Grest and M. Murat, Macromolecules **26**, 3108 (1993).
[15] J. D. Weinhold and S. K. Kumar, J. Chem. Phys. **101**, 4312 (1994).
[16] S. Förster, E. Wenz, and P. Lindner, Phys. Rev. Lett. **77**, 95 (1996).
[17] P. Auroy, L. Auvray, and L. Leger, Phys. Rev. Lett. **66**, 719 (1991).
[18] P. Auroy, Y. Mir, and L. Auvray, Phys. Rev. Lett. **69**, 93 (1992).
[19] A. Karim, S. K. Satija, J. F. Douglas, J. F. Ankner, and L. J. Fetters, Phys. Rev. Lett. **73**, 3407 (1994).
[20] D. Perahia, D. G. Wiesler, S. K. Satija, L. J. Fetters, S. K. Sinha, and S. T. Milner, Phys. Rev. Lett. **72**, 100 (1994).
[21] J. B. Field, C. Toprakciogly, L. Dai, G. Hadziioannou, G. Smith, and W. Hamiltan, J. Phys. (France) II **2**, 2221 (1992).
[22] H. J. Taunton, C. Toprackciogly, L. J. Fetters, and J. Klein, Macromolecules **23**, 571 (1990).
[23] R. M. Overney, D. P. Leta, C. F. Pictroski, M. H. Rafailovich, Y. Liu, J. Quinn, J. Sokolov, A. Eisenberg, and G. Overney, Phys. Rev. Lett. **76**, 1272 (1996).
[24] J. L. Anderson, P. F. McKenzie, and R. M. Webber, Langmuir **7**, 162 (1991).
[25] R. M. Webber, C. C. van der Linden, and J. L. Anderson, Langmuir **12**, 1040 (1996).
[26] A. A. Potanin and W. B. Russel, Phys. Rev. E **52**, 730 (1995).
[27] P. Y. Lai and K. Binder, J. Chem. Phys. **98**, 2366 (1993).
[28] J. Klein, E. Kumacheva, D. Mahalu, D. Perahia, and L. J. Fetters, Nature (London) **370**, 634 (1994).
[29] J. Klein, E. Kumacheva, D. Malahu, and D. Perahia, Macromol. Symp. **98**, 1149 (1994).
[30] R. S. Parnas and Y. Cohen, Rheol. Acta **33**, 485 (1994).
[31] Y. Rabin and S. Alexander, Europhys. Lett. **13**, 49 (1990).
[32] J. Klein, Colloids Surf. A **86**, 63 (1994).
[33] G. Sauerbrey, Arch. Elektrotech. Übertragung **18**, 617 (1964).
[34] F. Eggers and T. Funck, J. Phys. E **20**, 523 (1987).
[35] V. E. Granstaff, and S. J. Martin, J. Appl. Phys. **75**, 1319 (1994).
[36] D. Johannsmann, K. Mathauer, G. Wegner and W. Knoll, Phys. Rev. B **46**, 7808 (1992).
[37] A. Domack and D. Johannsmann, J. Appl. Phys. **80**, 2599 (1996).
[38] J. Rühe, Nachr. Chem. Tech. Lab. **42**, 1237 (1994).
[39] J. Rühe, Habilitation thesis, Universität Bayreuth, 1995 (unpublished).
[40] O. Prucker, Ph.D. thesis, Universität Bayreuth, 1995 (unpublished).
[41] G. Tovar, S. Paul, W. Knoll, O. Prucker, and J. Rühe, Supramol. Sci. **2**, 89 (1995).
[42] *Polymer Handbook*, 3rd ed., edited by J. Brandrup and E. H. Immergut (Wiley, New York, 1989), pp. VII, 175.
[43] A. Halperin, J. Phys. (France) **49**, 547 (1988).
[44] T. Nakamoto and T. Moriizumi, Jpn. J. Appl. Phys. **29**, 963 (1990).
[45] D. Johannsmann, J. Grüner, J. Wesser, K. Mathauer, G. Wegner, and W. Knoll, Thin Solid Films **210/211**, 662 (1992).
[46] D. Johannsmann, Ph.D. thesis, Universität Mainz, 1991 (unpublished).
[47] Strictly speaking, the refractive index $n=\varepsilon^{1/2}$ is the inverse of the optical impedance, which is $(\mu/\varepsilon)^{1/2}$, the magnetic permeability μ being constant in optics.
[48] R. M. A. Azzam and N. M. Bashara, *Ellipsometry and Polarised Light* (Elsevier, Amsterdam, 1987).
[49] Z. X. Lin and M. D. Ward, Anal. Chem. **67**, 685 (1995).
[50] V. E. Bottom, *Introduction to Quartz Crystal Unit Design* (Van Nostrand Reinhold, New York, 1982).
[51] J. D. Ferry, *Viscoelastic Properties of Polymers* (Wiley, New York, 1980).
[52] J. L. Harden and M. E. Cates, Phys. Rev. E **53**, 3782 (1996).
[53] M. Aubouy, J. L. Harden, and M. E. Cates, J. Phys. (France) II **6**, 969 (1996).
[54] G. S. Grest, Phys. Rev. Lett. **76**, 4979 (1996).
[55] G. H. Peters and D. J. Tildesley, Phys. Rev. E **52**, 1882 (1995).
[56] C. Yeung, A. C. Balazs, and D. Jasnow, Macromolecules **26**, 1914 (1993).
[57] K. G. Soga, Hong Guo, and M. J. Zuckermann, Europhys. Lett. **29**, 531 (1995).
[58] P. W. Zhu, D. Napper, J. Colloid Interface Sci. **164**, 489 (1994).
[59] S. Paul, O. Prucker, N. Bunjes, J. Habicht, J. Rühe, and W. Knoll (unpublished).
[60] L. I. Klushin and A. M. Skvotrsov, Macromolecules **25**, 3443 (1992).
[61] S. T. Milner, T. A. Witten, and M. E. Cates, Macromolecules **22**, 853 (1989).
[62] A. Sahnoune, F. Massines, and L. Piche, J. Polym. Sci. B **34**, 341 (1996).
[63] H. Nomura, S. Kato, and Y. Miyahara, J. Soc. Mater. Sci. Jpn. **22**, 434 (1973).
[64] M. Doi and S. F. Edwards, *The Theory of Polymer Dynamics* (Clarendon, Oxford, 1986).
[65] P. F. Mijnlieff and W. J. M. Jaspers, Trans. Faraday Soc. **67**, 1837 (1971).